Thermal conductivity and localization in glasses: Numerical study of a model of amorphous silicon

Joseph L. Feldman and Mark D. Kluge
Complex Systems Theory Branch, Naval Research Laboratory, Washington, D.C. 20375-5000

Philip B. Allen
Department of Physics, State University of New York, Stony Brook, New York 11794-3800

Frederick Wooten
Department of Applied Science, University of California at Davis/Livermore, Livermore, California 94550
(Received 12 January 1993; revised manuscript received 6 July 1993)

Numerical calculations of thermal conductivity $\kappa(T)$ are reported for realistic atomic structure models of amorphous silicon with 1000 atoms and periodic boundary conditions. Using Stillinger-Weber forces, the vibrational eigenstates are computed by exact diagonalization in harmonic approximation. Only the uppermost 3% of the states are localized. The finite size of the system prevents accurate information about low-energy vibrations, but the 98% of the modes with energies above 10 meV are densely enough represented to permit a lot of information to be extracted. Each harmonic mode has an intrinsic (harmonic) diffusivity defined by the Kubo formula, which we can accurately calculate for $\omega > 10$ meV. If the mode could be assigned a wave vector $\mathbf{k}$ and a velocity $\mathbf{v}=\partial\omega/\partial\mathbf{k}$, then Boltzmann theory assigns a diffusivity $D_{\mathbf{k}}=\frac{1}{3}vl$, where l is the mean free path. We find that we cannot define a wave vector for the majority of the states, but the intrinsic harmonic diffusivity is still well-defined and has a numerical value similar to what one gets by using the Boltzmann result, replacing v by a sound velocity and replacing l by an interatomic distance a. This appears to justify the notion of a minimum thermal conductivity as discussed by Kittel, Slack, and others. In order to fit the experimental $\kappa(T)$ it is necessary to add a Debye-like continuation from 10 meV down to 0 meV. The harmonic diffusivity becomes a Rayleigh ω^{-4} law and gives a divergent $\kappa(T)$ as $T\rightarrow 0$. To eliminate this we make the standard assumption of resonant-plus-relaxational absorption from two-level systems (this is an anharmonic effect which would lie outside our model even if it did contain two-level systems implicitly). A reasonable fit and explanation then results for the behavior of $\kappa(T)$ in all temperature regimes. We also study the effect of increasing the harmonic disorder by substitutional mass defects (modeling amorphous Si/Ge alloys). The additional disorder increases the fraction of localized states, but delocalized states still dominate. However, the diffusivity of the delocalized states is diminished, weakening our faith in any literal interpretation of the minimum conductivity idea.

I. INTRODUCTION

The thermal conductivity κ of amorphous silicon (a-Si) has recently been measured.[1,2] Two factors make this an attractive case for detailed theoretical study. First, a-Si has technological applications, and especially for potential thermoelectric applications, a deeper understanding of thermal conductivity might be important. Second, from a purely theoretical point of view, a-Si can be used as a model system for studying generic effects seen in κ of glasses. Figure 1 shows the experimental data, and also our theoretical fits explained in Sec. III. The behavior of $\kappa(T)$ is customarily classified into three regimes: (1) At low temperatures, where only low-energy vibrations are excited, $\kappa(T)$ is approximately[3] a quadratic function of T. The model of scattering from two-level systems[4] seems to give a satisfactory fit. Our theory adds nothing to the conventional view of this regime. (2) At somewhat higher temperatures, typically 10–30 K as seen in Fig. 1, there is a "plateau" region. (3) At $T > 30$ K, $\kappa(T)$ rises smoothly to a T-independent final or "saturated" value. In this last regime, we believe that the dominant mechanism is the intrinsic harmonic diffusion of higher-energy delocalized vibrations. These modes have not been well described by most previous theories. It is also our belief that most of the effects seen in $\kappa(T)$ of glasses have close analogs in electrical transport of disordered metals; this provides a third motivation for our study.

The vibrations which dominate the high-T heat transport in our theory lie near the borderline of Anderson localization. However, except for a small minority ($\approx 3\%$), the vibrational eigenstates are *not* localized. Neither are they "propagating," that is, there is no sensible way to assign a wave vector or velocity. Nevertheless, they carry heat, contributing to $\kappa(T)$ an amount $C_i(T)D_i/V$ per mode i, where the specific heat C_i is k_B at high T and D_i is a temperature independent "mode diffusivity" defined in the previous paper.[5] Boltzmann transport theory (which is *not* applicable) would have given $D_i=v_i l_i/3$. As observed by Kittel,[6] if the sound velocity is used instead of v_i and the interatomic spacing is used instead of the mean free path l_i, then $\kappa(T)$ is qualitatively and semiquantitatively fit at temperatures above the plateau region. Slack[7] has discussed how such a mod-

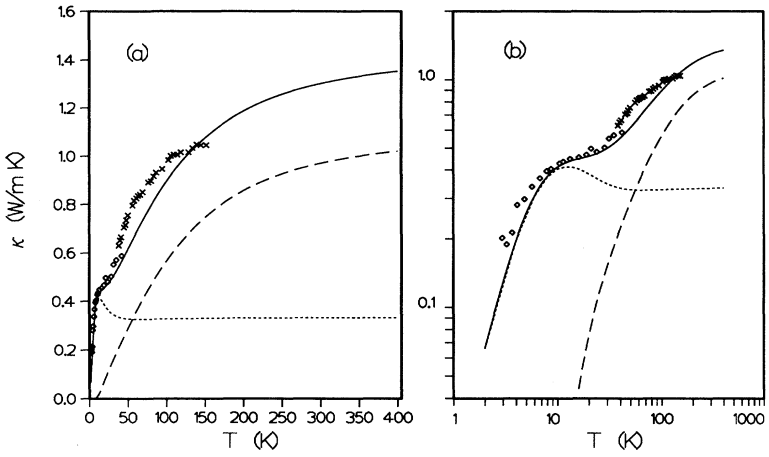

FIG. 1. Thermal conductivity vs temperature in amorphous Si. Diamonds are data from Ref. 1, ×'s are from Ref. 2. Lines are our theoretical fits discussed in Sec. III. In addition to the total $\kappa(T)$ (solid line), the theoretical contributions are shown separately from vibrations with energies above (long dashed line) and below (short dashed line) 5 meV.

el is also useful for crystalline insulators with strong scattering. In this paper we report numerical calculations on realistic finite size models which explain why this picture is qualitatively sensible, and agree well enough with experiment to support this picture. This picture is also supported by recent simulation results of Sheng and Zhou,[8] and by a phenomenological analysis of Love and Anderson.[9] Our work does *not* ignore localization. Our system sizes are large enough that the location of the mobility edge is relatively precise and unambiguous. Both the standard participation ratio calculation, and the D_i calculation show a sharp breakpoint at the onset of localized states, where D_i becomes zero *modulo* exponentially small finite-size errors. Our theory stays within harmonic approximation, and therefore there are no inelastic processes which could permit localized states to carry heat at any temperature. Thus our theory of heat conduction is in explicit opposition to models of hopping between localized states proposed by various authors.[10,11] The accuracy of the harmonic restriction depends on the material under consideration. In an early simulation, Payton, Rich, and Visscher[12] saw evidence that turning on anharmonicity increased the value of κ at higher T. However, silicon in crystalline form is very harmonic (its thermal conductivity rivals Cu at room temperature, and exceeds it at nitrogen temperature). In spite of an argument to the contrary by Michalski,[11] we see no reason why the amorphous state should greatly enhance anharmonic interactions (except for the "two-level-system" effects which are intrinsically anharmonic, but very dilute and important only at low T). Our preliminary classical simulations of a-Si with the fully anharmonic Stillinger-Weber (SW)[13] potential confirm that anharmonic effects are weak in this model.

There is a common notion that eigenstates are either propagating or localized, and that states near the margin of localization cannot give very large transport currents, perhaps because the regime near the margin is presumed to be narrow. Further, it is sometimes taken to be obvious that most vibrational states in glasses are localized. As an example, Jagannathan, Orbach, and Entin-Wohlman[10] mention ". . . a theoretical consensus that the Ioffe-Regel condition signals localization." The "Ioffe-Regel condition" means $l \approx a$, i.e., states not propagating, and is ubiquitous in glasses. Our calculation demonstrates that the identification of the Ioffe-Regel condition with localization is wrong. We find only a narrow region of localized states at high frequencies, but a wide region where the Ioffe-Regel condition is obeyed, with enough heat transport in these nonpropagating delocalized states to explain the experimental $\kappa(T)$ at temperatures above the plateau. A similar situation applies in the case of electron eigenstates in metallic glasses or disordered alloys, and it is worth presenting the arguments because electrons are in one sense simpler. In principle, vibrations can never completely localize (the long wavelength hydrodynamic modes always can propagate) whereas the relevant electrons within $\sim 10k_B T$ of the Fermi level of a metal can in principle all localize. An "Anderson heat insulator" is forbidden, but an "Anderson electrical insulator" is not. Very disordered metals often have resistivities within a factor of 2 of 150 $\mu\Omega$ cm and show very little T dependence. This is just the value that emerges when each one-electron state has a diffusivity $v_F l/3$ and l is set equal to a lattice constant a, i.e. it is the Ioffe-Regel condition. These one-electron states are *not* localized, as can be deduced from three different experimental observations. (1) The resistivity does not diverge as $T \rightarrow 0$ but instead remains almost independent of T. (2) At higher T the resistivity is still T independent, whereas conduction in localized states should improve as T increases because of thermally activated hopping and also possible thermal activation of carriers into delocalized states. (3) The overwhelming majority of these metals cannot be made into Anderson insulators by any form of abuse (alloy substitutions or radiation damage) except diluting them severely with very nonmetallic elements like Ar. Appropriating somewhat loosely the language of attractors and fixed points, under a wide range of disordering conditions, both electrical conductors and electrically insulating heat conductors collect at the *"diffusive fixed point"* where they are neither Anderson insulators nor quasiparticle conductors. This is probably not a mathematical fixed point of a well-defined class of Hamiltonians, but instead a phenomenological fixed point (much as the notion of a Fermi liquid as a physical fixed point seems more

general than can yet be warranted by the scaling properties of real Hamiltonians).

The usefulness of Si as a model system derives from the fact that there are microscopic models for interatomic forces and for atomic coordinates, both of which are needed for microscopic theory. In most ways we believe *a*-Si can be considered a typical glass. Some people reserve the word "glass" for systems which can be produced in bulk rather than only thin film form, but we believe that this distinction refers simply to relative heights of energy barriers to recrystallization, and has no fundamental importance for our considerations. In one respect, *a*-Si may not be a typical glass. The linear term γT in the specific heat (seen at very low T in *a*-Ge) disappears in a large B field.[14] Apparently the linear term is caused by nearly free spins at dangling bonds, loosely coupled to neighboring spins to form singlet and triplet states with random splittings. The contribution to γ from "two level systems" is apparently suppressed by at least an order of magnitude in *a*-Ge and probably also *a*-Si. The similarity of $\kappa(T)$ in Fig. 1 to the "universal" behavior of other glasses shows that this difference is probably not important.

The previous paper[5] (hereafter denoted by AF) gives the formalism, i.e., the use of exact harmonic eigenstates of specific disordered atomistic models containing N atoms with periodic boundary conditions. The resulting $3N$ eigenfrequencies ω_i and eigenvectors ϵ_i are used to evaluate the Kubo formula for κ. This paper is organized as follows. Section II describes the network models for *a*-Si. Section III presents our fit to the thermal conductivity of amorphous Si which has already been seen in Fig. 1. Three fitting parameters are used to described inelastic effects necessary for the low-frequency vibrations. Higher-frequency vibrations are only weakly influenced by these inelastic processes, and their intrinsic harmonic diffusivity dominates. This part of the calculation has no adjustable parameters. The computation of the intrinsic harmonic effects is described somewhat superficially in Sec. III, but further details are given in Sec. IV, devoted to finite-size effects. Specifically, we examine the dependence of calculated values of $\kappa(T)$ upon N, upon the choice of boundary conditions at the edges of the unit cell, and upon the direction of heat flow. The method of extrapolation to zero frequency is discussed. The problematic contribution of low-frequency modes to κ is evident in Sec. IV, but is cured by the phenomenological treatment of inelastic processes given in Sec. III. Section V contains calculations of spectral functions which illuminate the question of the assignment of a wave vector and a mean free path to a vibrational eigenstate. Section VI presents new results for mass-disordered amorphous $Si_{1-x}Ge_x$ alloys, and hypothetical alloys with even larger mass disorder. These results shed light on the concept of minimum thermal conductivity and the transition from delocalized to localized vibrational eigenstates.

II. NETWORK MODELS FOR AMORPHOUS SILICON

The atomic coordinates are vertices of random tetrahedral networks containing $8n^3$ atoms in a large cube of side $n \times a$, where $a = 5.515$ Å. The networks obey periodic boundary conditions with period na (1,0,0), etc., and are constructed starting from the crystalline diamond structure, using the bond interchange algorithm of Wooten, Winer, and Weaire (WWW).[15] During the implementation of this algorithm, the Keating potential[16] is used to relax atomic coordinates. After the network is built, we make a further relaxation to the nearest local minimum of the Stillinger-Weber (SW)[13] potential. Force constants are taken from derivatives of the SW potential. The Keating potential would not be very satisfactory for this purpose, because unlike SW it is intended only for small deviations away from perfect tetrahedral coordination. Even more than the original WWW models, our SW-relaxed WWW models contain significant deviations from perfection, including occasional (of order 2%) local fivefold coordination, and the SW potential is designed to give realistic forces under such circumstances. Cowley[17] has shown that SW forces are reasonably good for bulk crystalline Si, and Li *et al.*[18] showed that SW forces still gave reasonable vibrations on the highly distorted 7×7 reconstructed (111) surface. We reported earlier results for an $n = 3$, $N = 216$ atom model,[19] and then for an incompletely relaxed $n = 5$, $N = 1000$ atom model.[20] In this paper, more complete results are given for a completely relaxed $N = 1000$ atom model. Further details are in Sec. IV.

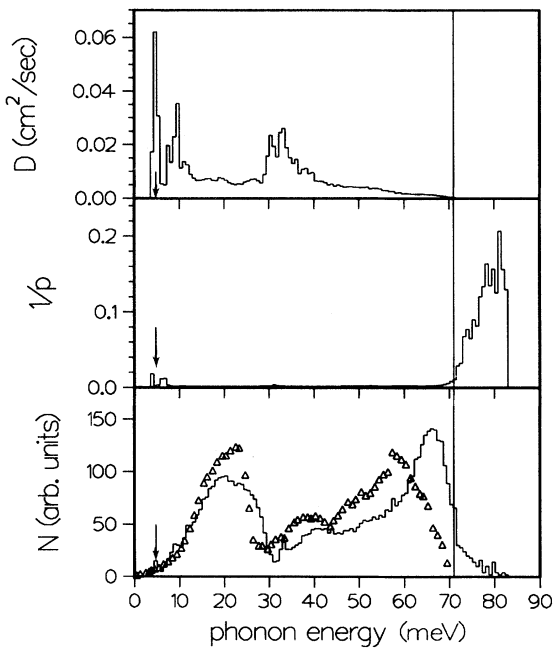

FIG. 2. Vibrational density of states $N(\omega)$ of amorphous Si. Data are from Ref. 22. Theoretical values are compiled from 3000 eigenfrequencies calculated with periodic boundary conditions ($\mathbf{Q}=0$) and 3000 eigenfrequencies calculated with antiperiodic boundary conditions [$\mathbf{Q}=(\pi/5a)(1,1,1)$]. Also shown are mode diffusivities and inverse participation ratios as discussed in Sec. III. The vertical line at 71 meV shows the location of the mobility edge. The arrows locate the frequency of the propagating mode of minimum energy, whose wavelength is twice the diagonal of our 28 Å cell.

Although we believe our model to be as good as any available, there is no way to claim that it accurately represents real amorphous Si. The actual microstructure depends somewhat on the synthesis, and important details are still under discussion.[21] We only claim that our model is a very sensible network model. Also, the subject of interatomic forces in Si is not settled. We only claim that the SW forces are neither pathological nor unphysical. A measure of the realism of our model is shown in Fig. 2 which gives the vibrational density of states compared with neutron-scattering experiments by Kamitakahara *et al.*[22] The mathematical definition

$$N(\omega)=\sum_i \bar{\delta}(\omega-\omega_i) \tag{1}$$

was used, where $\bar{\delta}$ is a rectangular approximation to a δ-function centered at discrete frequencies ω with width equal to 0.715 meV. The energy of the upper end of the spectrum is overestimated by about 20%. This seems to be a fault of the SW potential, rather than of the WWW procedure for generating structural models. The SW model makes the same overestimate when applied to crystalline Si.[18] Compared with the crystalline case, *a*-Si has a fairly similar phonon density of states, the most important difference being the softening of the lowest-energy peak in the amorphous material.

III. PURE AMORPHOUS SILICON

The central result of our theory is the intrinsic harmonic diffusivity D_i, defined in Eq. (22) of AF, and shown in Fig. 2. Actually, Fig. 2 shows D_i averaged over modes in a frequency interval similar to Eq. (1), that is,

$$D(\omega)=\sum_i D_i \bar{\delta}(\omega-\omega_i)/N(\omega) \ . \tag{2}$$

In order to calculate D_i for a finite system where the eigenfrequencies are discrete rather than infinitely dense, it is necessary to use in Eq. (22) of AF a broadened δ function with a width greater than the level spacing. In principle, the width of the δ function goes to zero after the system size goes to infinity. We have used a Lorentzian of width 0.0429 meV. The resulting values of D_i showed large fluctuations [rms fluctuations of $\sim$25% within the bins used in Eq. (2)]. A larger width of the Lorentzian would probably have diminished these fluctuations, but the interesting possibility exists that in the infinite-size limit, the value of D_i has significant random fluctuations from state to state, reflecting the idiosyncratic nature of these delocalized but nonpropagating states. In any event, they average out smoothly in Eq. (2) and Fig. 2.

There are two regions of large diffusivity, the lowest frequencies, and the region around 35 meV. In crystalline Si, this second region is a portion of the spectrum above the transverse acoustic vibrations, where longitudinal modes have large velocities and are probably very effective carriers of heat. The reason for the high diffusivity in the amorphous state is that there is a local minimum in the density of states, so that the structural disorder mixes these pseudolongitudinal vibrations with relatively few other modes, preserving something of their propagating character. Perhaps it is possible to assign these modes a velocity and mean free path. As a crude estimate, set the diffusivity $D\approx 2\times 10^{-6}$ m^2/s equal to $\frac{1}{3}vl$ and choose for v the longitudinal sound velocity found for this same model of *a*-Si, $v_L=7.64\times 10^3$ m/s.[23] This yields an estimated mean free path of 8 Å (safely smaller than our 28 Å cell size) for this especially diffusive region of the spectrum. With such a short mean free path, the notions of wave vector, velocity, and mean free path can only be marginally meaningful.

Above 40 meV there is a smooth decrease of diffusivity, approximately linear in energy [$D_i \propto (\omega_c-\omega_i)^p$ with a critical exponent $p\approx 1$] and a critical energy $\omega_c=71$ meV where D_i vanishes to within a very small noise level. The critical exponent of 1 agrees with scaling and other theories of Anderson localization,[24] and we believe that this locates the mobility edge above which the diffusivity would be strictly zero in the infinite size limit. As a further test of this, we have calculated the "inverse participation ratio" $1/p_i$, defined as

$$\frac{1}{p_i}=\sum_l \left[\sum_\alpha \epsilon_i(l,\alpha)^2\right]^2 , \tag{3}$$

where $\epsilon_i(l,\alpha)$ is the αth Cartesian component of the normalized polarization vector of the ith mode on the lth atom. The square of this polarization vector when summed over all atoms gives 1. Here it is squared a second time before summing. If the vibration were localized on a single atom, the result would still be 1, whereas if the vibration were equally distributed on all atoms, the result would be $1/N$. Thus p_i measures n_i, the number of atoms on which the ith vibrational mode has significant amplitude. For a delocalized mode, $1/p_i\to 0$ as the system size $\to\infty$, whereas for localized mode, $1/p_i$ remains nonzero. Figure 2 shows a sharp increase in $1/p_i$ at $\omega_i=71$ meV, just where the diffusivity approaches zero. The 3% of eigenstates above this energy seem very clearly to be localized. On the scale of our cell size (28 Å) 97% of the phonons are delocalized. We think that this estimate is not sensitive to system size, or to fine details of the structural model. The same result holds for both smaller 216-atom models, and has been confirmed by Biswas *et al.*[25] We believe that this is the normal situation for vibrations in glasses, provided that they are reasonably dense, i.e., not too porous.

There are possibly a very few localized modes at $\omega_i=31$ meV, where there is a sharp minimum in the density of states separating the low-energy transverse peak from higher-energy modes. The lowest nonzero mode also appears localized, an effect also seen by Biswas *et al.*[25] The energy of this mode is 4.15 and 4.11 meV for periodic and antiperiodic boundary conditions, respectively. Based on the inverse participation ratio, this mode involves roughly 21 and 53 atoms (of the 1000 atoms in the model) for periodic and antiperiodic boundary conditions, respectively. (Given the sensitivity of the inverse participation ratio to the boundary conditions it is clear that this mode is not completely localized within the scale of the model.) It seems likely that this is a

finite-size effect. In a larger system, there would be more modes in this energy region. Probably these modes would be pseudoacoustic progagating modes. At the lowest energy, finite-size effects, even for large model systems, will cause an unphysical gap at the bottom of the spectrum, and the states closest to this gap might be or appear to be localized in the finite-size theory, although not localized but propagating (and maybe resonant) in a macroscopic sample. It is well documented by specific heat and neutron scattering[26] that glasses have "extra" low-energy modes. These are probably related to defects or "soft" parts of the sample, and are unlikely to be correctly incorporated in our model. In particular, we do not think they account for the small peaks in $1/p$ seen at low energies in Fig. 2.

Now we are ready to calculate $\kappa(T)$, using the standard result

$$\kappa(T)=\int_0^{\omega_{\max}} \frac{d\omega\, N(\omega)C(\omega/T)D(\omega)}{V} , \tag{4}$$

$$C(\omega/T)=k_B \left[\frac{\hbar\omega/2k_BT}{\sinh(\hbar\omega/2k_BT)} \right]^2 , \tag{5}$$

where the last formula is the specific heat of an oscillator of energy ω. The results are shown as the middle curve in Fig. 3. There is a significant finite-size problem in this theory which will be discussed both here and in the next section. By inspection of Fig. 2 it is obvious that we have

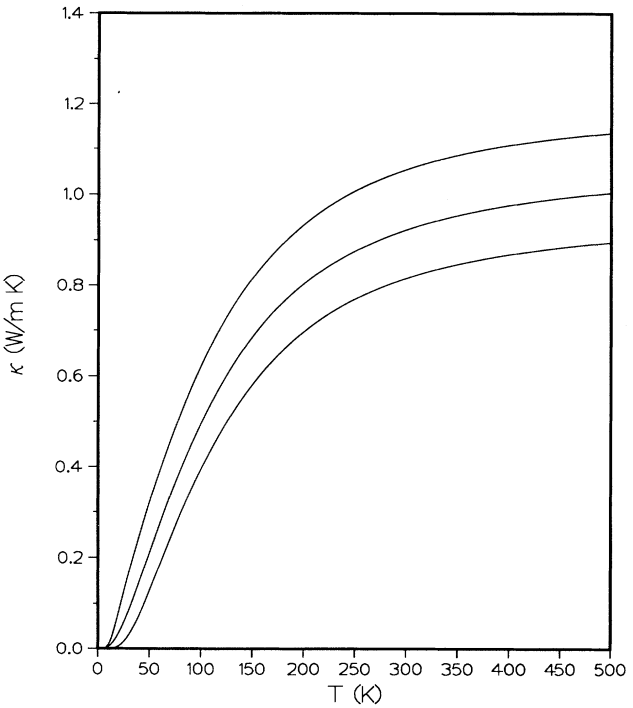

FIG. 3. Thermal conductivity vs temperature for amorphous Si. The middle curve comes from integrating the numerical $N(\omega)$ and $D(\omega)$ curves of Fig. 2; the lower curve is the same with the integrals cut off at a lower frequency of 10 meV; the upper curve has $N(\omega)$ and $D(\omega)$ smoothly continued to low ω but the integrals cut off below 5 meV.

very poor statistics for properties of modes with $\omega < 10$ meV. Although the density of states $N(\omega)$ is small, the diffusivity $D(\omega)$ is big, and the heat capacity for all but low T is saturated at its biggest value k_B. The product $N(\omega)D(\omega)$ is not small and is fluctuating badly because of poor statistics arising from the finite system size. The nature of the problem is worsened when one realizes that, in principle, the harmonic diffusivity at low ω is a property of propagating modes which must obey a Rayleigh law $D(\omega)\propto\omega^{-4}$ at low ω, and this is sufficiently singular that the integral (3) for $\kappa(T)$ diverges at all T. (For an imaginary harmonic material, the divergence is cut off by the system size, and κ will scale as $L^{1/4}$.) This property of harmonic systems is well known,[27] although it is perhaps surprising to realize that it applies not just to weakly disordered crystalline matter, but also to strongly disordered amorphous material.

One way to estimate the importance of the low-ω region is to replace the low-ω parts of $N(\omega)$ and $D(\omega)$ in Fig. 2 by appropriately chosen smooth extrapolations. For the density of states, we used a Debye extrapolation, $N(\omega)=C_D\omega^2$ with the coefficient C_D determined by the sound velocities $v_L=7.64\times10^3$ m/s and $v_T=3.67\times10^3$ m/s previously calculated for this model.[23] This not only matches nicely with the numerical results at $\omega\approx11$ meV, but also fits fairly well with the measure T^3 specific heat[29] (the corresponding theoretical Debye temperature is 446 K, while specific heat gives 528±20 K). To extrapolate $D(\omega)$ is far more dangerous because there are no firm guidelines, but we will see later that the method is not very important. Therefore, we arbitrarily chose the Rayleigh ω^{-4} law and used it to continue smoothly onto our calculation at $\omega=11$ meV where $D(\omega)$ first becomes smooth. Figure 3 shows three curves. The middle one is just the raw calculation which is uncontrolled at low ω. The upper one is the calculation using the smooth continuation just described for $D(\omega)$ and $N(\omega)$, but with a lower frequency cutoff of 5 meV to avoid the divergence. The lowest curve is the integral of the raw calculations, but with a lower cutoff of 10 meV which avoids the region where the calculation is uncontrolled. These results show that the low-ω region in harmonic theory is making a significant contribution to $\kappa(T)$ at all T.

Real materials always have anharmonic interactions, and even the mild anharmonicity of crystalline matter is sufficient to cure the divergence. However, glassy materials have anomalously small low-T conductivity, which requires an exceptionally effective inelastic process. The accepted description involves scattering from "two-level systems" (TLS). Since atomic TLS's seem scarcer in a-Si (Ref. 14) than in most glasses, the inelastic mechanism may be different, for example, perhaps the spin singlet-triplet systems causing the linear specific heat are scattering the low-energy vibrations.

At ω low enough that modes propagate and a Boltzmann description applies, the usual lowest-order treatment gives Mattheissen's rule, that is, a summation of the various resistive mechanisms:

$$\frac{1}{D(\omega)}=\frac{1}{D_h(\omega)}+\frac{1}{D_{\rm res}(\omega,T)}+\frac{1}{D_{\rm rel}(\omega,T)} . \tag{6}$$

The first term is the intrinsic harmonic term which we calculate numerically at higher ω and continue smoothly at lower ω. Since the last two terms dominate at low ω, the answers should not be sensitive to the extrapolation procedure used for D_h. The second term refers to resonant absorption where a propagating vibration of energy ω is absorbed by a TLS of energy splitting ω which is initially in its lower-energy state:

$$\frac{1}{D_{\rm res}(\omega,T)}=d_{\rm res}^{-1}\frac{\hbar\omega}{k_B T_0}\tanh\frac{\hbar\omega}{2k_B T} . \tag{7}$$

The third term refers to absorption by structural relaxation processes. Although logically independent of the second term, TLS's give one mechanism of relaxational absorption. In the regime where the phonon-induced TLS flipping rate is greater than its energy splitting, the environmental damping has destroyed the simple two-level problem. Vibrational modes perceive this as a classical viscous damping. Hunklinger and Arnold[28] summarize a unified theory of these effects, which yields a complicated formula for the additional absorption due to relaxational effects. A simplified version of this formula is

$$\frac{1}{D_{\rm rel}(\omega)}=d_{\rm rel}^{-1}\frac{(T/T_0)^3}{1+(k_B T_0/\hbar\omega)(T/T_0)^3} . \tag{8}$$

This form was used by Sheng and Zhou,[8] with the additional constraint that the coefficients $d_{\rm rel}$ and $d_{\rm res}$ had the ratio 2. We see little reason for this constraint and use three independent adjustable parameters, $T_0=20$ K, $d_{\rm rel}=2.5\times10^{-4}$ m^2/s, and $d_{\rm res}=1.7\times10^{-4}$ m^2/s. The ratio is remarkably close to 2; fixing the ratio at 2 would not much affect the quality of the fit to experiment.

Although the Mattheissen's rule form is only justified for the low-frequency propagating modes, the extra inelastic terms in Eq. (6) are fairly unimportant at higher ω where the harmonic resistivity is large (D_h is small). Therefore, there is no harm in using the form of Eq. (6) for all frequencies. The results are shown in Fig. 1. Also shown are the separated contributions of the frequencies above and below 5 meV. The contribution from above 5 meV should be compared with the upper curve of Fig. 3, which is the same thing without the additional inelastic terms, and therefore slightly larger.

An interpretation of the plateau phenomenon can now be offered which is only slightly oversimplified. As seen by Figs. 1 and 3, the total thermal conductivity can be thought of as the sum of two different conduction channels. The first, which dominates at low T, is heat carried in a conventional way by propagating long wavelength acoustic modes, scattering strongly from the special inelastic processes available in a glass. These processes kill off the low-frequency contribution at higher temperatures, leaving a peak at $\approx$20 K which becomes the plateau. The second channel, although less familiar, is quite elementary. It is the heat carried by nonpropagating modes which are strongly influenced by the glassy disorder but mostly not localized and therefore able to conduct by intrinsic harmonic diffusivity. This is a very smooth term which closely resembles the specific heat and saturates like the specific heat at high T. Following Slack[7] we could call this piece the "minimum thermal conductivity." The sum of these terms will produce a plateaulike feature for a fairly broad range of parameters. This picture is a sort of "shunt-resistor model," reminiscent of the model which has often been used to describe the resistivity of metals with strong electron-phonon scattering.[30] When the propagating modes become reasonably well damped and are no longer able to carry much heat, the great reservoir of delocalized and poorly conducting vibrations (the "shunt") takes over, giving a net result in good accord with Kittel's old picture.

Precisely the same explanation of thermal conductivity was given by Sheng and Zhou,[8] and even earlier by us[19] in a short communication about this work. The work of Sheng and Zhou used a less realistic model, but calculated diffusivities by direct simulation which enabled larger systems to be explored. It also seems to us that the simulations by Michalski[11] largely support this picture, but have been misinterpreted as providing support for the picture of Jagannathan, Orbach, and Entin-Wohlman.[10] On the other hand, the notion of "minimum conductivity" still has no strong theoretical basis. The results of this section simply show that the nature of thermal conduction in a-Si is consistent with and adequately described by this notion. In Sec. VI we present further calculations to test the limits of this notion, and learn that it is not very robust or absolute. Nevertheless, it is undeniable that, from an experimental point of view, "minimum thermal conductivity" is a very real effect (see, for example, a recent study of disordered crystals by Cahill, Watson, and Pohl[31]). We conclude that it is a real effect with a fuzzy explanation, namely, that the crossover from propagating to localized is gradual enough that many real materials are found in the crossover region.

IV. SIZE EFFECTS

Invoking the shunt-resistor picture, we see that it is possible to calculate the intrinsic harmonic diffusive conductivity contributed by higher-frequency modes, using finite-size systems, and exact diagonalization methods. From now on we will discuss only this contribution to the conductivity, on the assumption that it dominates $\kappa(T)$ at higher T; the remaining contribution can be estimated and tacked on if desired. The present section provides further details about these calculations.

In order to document the effect of system size on our calculations, this section compares previous results[19] for the 216-atom model[15] with new results for the 1000-atom model described in Sec. II. Also, a second 216-atom model is introduced her for comparison. This new model is denoted by 216b to distinguish it from the previous model, denoted by 216a. All three models have been relaxed to a minimum of the SW potential. Model 216a used the original WWW coordinates, while models 216b and 1000 were created using the same algorithm except without prohibition of fourfold rings. Before relaxation with the SW potential, model 216b had six fourfold rings, and model 1000 had 19. After relaxation, these numbers did not change, but a few threefold and fivefold coordi-

nated atoms appeared. The density of models 216b and 1000 is about 2% less than model 216a which in turn is about 2% less than crystalline Si.

Figure 4 shows the frequency-dependent κ for the 1000-atom model at $T=175$ K, evaluated using the formula

$$\kappa_{xx}(\omega)=\frac{V}{T}\sum_{ij}\frac{n_j-n_i}{\hbar(\omega_i-\omega_j)}|\langle i|S_x|j\rangle|^2 \times\frac{\eta}{(\omega_i-\omega_j-\omega)^2+\eta^2}\ . \quad (9)$$

This is just Eq. (20) of AF with the delta function broadened into a Lorentzian of width $\eta=0.043$ meV. The eigenfrequencies ω_i and eigenvectors $|i>$ are found by diagonalization of the 648×648 or 3000×3000 dynamical matrices using the IBM 3090 at the Cornell Supercomputer Center. The force constants in the dynamical matrices are derivatives of the SW potential energy. The heat current matrix elements $\langle i|S_x|j\rangle$ are calculated using Eq. (A7) of AF. To diminish the statistical noise, Fig. 4 shows the average of κ_{xx}, κ_{yy}, and κ_{zz}. The separate $\kappa_{\alpha\alpha}(\omega)$ curves agree well with each other for $\alpha=x$, y, and z. For 216-atom models, the size of the random differences between, e.g., κ_{xx} and κ_{yy} are a few percent of κ, and also the off-diagonal elements like κ_{xy} are a few percent of κ. This shows that our model is isotropic at a level of accuracy equal or better than the other sources of finite size error. The two curves of Fig. 4 are

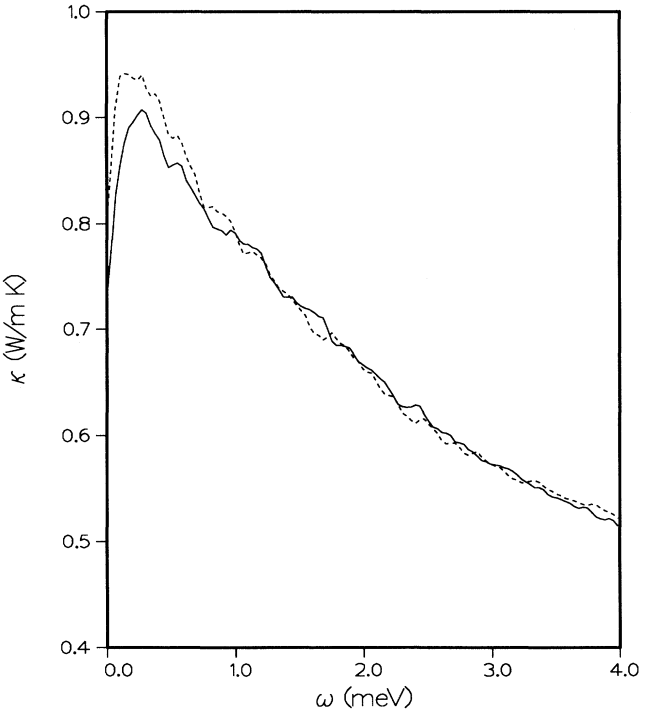

FIG. 4. Thermal conductivity vs frequency for the 1000-atom model of a-Si, calculated at $T=175$ K. The solid curve shows the result with periodic ($\mathbf{Q}=0$) boundary conditions, and the dashed curve shows the result with antiperiodic [$\mathbf{Q}=(\pi/5a)(1,1,1)$] boundary conditions.

results obtained for periodic and antiperiodic boundary conditions for the atom motions. Antiperiodic boundary conditions means that a displacement vector $-\mathbf{u}$ is assigned to the six equivalent atoms in the six face-sharing cubes if the displacement of the original atom is $\mathbf{u}$. This is the same as assigning a wave vector $\mathbf{Q}=(\pi/na)(1,1,1)$ to the "phonon" eigenstates which are found when the model is considered to be a crystal with an $n=5$, 1000-atom cell. Periodic boundary conditions correspond to $\mathbf{Q}=\mathbf{0}$. As can be seen from the figure, the results are relatively insensitive to the choice of boundary conditions. This property suggests that a 1000-atom cell is more than sufficiently large to describe the bulk behavior, at least at frequencies which are not too low. The sensitivity to boundary conditions is enhanced at small ω. The principal difference between $\mathbf{Q}=\mathbf{0}$ and $\mathbf{Q}=(\pi/na)(1,1,1)$ lies in the lowest modes. At $\mathbf{Q}=\mathbf{0}$, there are three zero-frequency eigenvalues which are uniform translations; the next modes up, apart from the previously mentioned quasilocalized one, are disordered versions of crystalline states which would have been transverse vibrations with wavevectors equal to $(2\pi/na)(1,0,0)$. Taking into account the six equivalent wave vectors, there are twelve such vibrational states, which all would be degenerate in a crystal, but are mixed and split by the structural disorder. The energies of the first nonzero eigenstates of our 1000-atom model are ≈5.1 meV. In our calculations of κ the modes of uniform translation are omitted. For antiperiodic boundary conditions, there are no $\omega=0$ modes of uniform translation, and the lowest-lying modes, apart from the quasilocalized one, are those which would have been transverse vibrations with wave vectors equal to $(\pi/na)(1,1,1)$ in a crystalline situation. There are 16 such modes in a crystal. The lowest energies of vibrations with antiperiodic boundary conditions in our 1000-atom model are ≈4.6 meV.

In the dc limit, the mechanism of heat conduction is transfer of energy between delocalized modes of equal energy by the heat current operator. For a finite disordered system, there are not any modes of precisely equal energy. Having no symmetry-allowed level crossings, the eigenstates tend to repel each other, and the typical level spacing is just $\omega_{\max}/3N$, or ≈0.01 meV. By broadening the delta function in Eq. (20) of AF by an amount proportional to the mean level spacing, a theory is obtained which converges to the desired answer in the $N\rightarrow\infty$ limit. We discover in our numerical work that the lowest-lying states carry a disproportionate amount of heat current. This can be seen from the fact that there is a small excess heat current in the case of antiperiodic boundary conditions, associated with the lower lying and more numerous pseudoacoustic modes.

Figure 5 compares the thermal conductivities of the 216- and 1000-atom models. From now on, all calculations of κ refer implicitly to results which are averages of xx, yy, and zz components and also averages of results for periodic and antiperiodic boundary conditions. The Lorentzian broadening parameter η was set to 0.17 meV for models 216a and 216b and to 0.043 meV for model 1000. At $\omega>1$ meV, models 216b and 1000 have a very satisfying agreement, while the topologically distinct

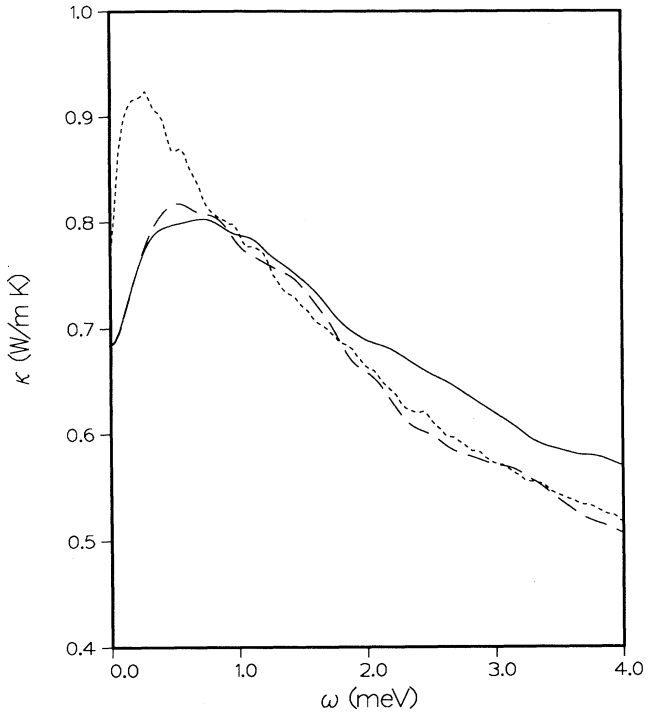

FIG. 5. Thermal conductivity vs frequency for three models of *a*-Si at 175 K. Solid line: model 216a; dashed line: model 216b; dotted line: model 1000.

model 216a (without fourfold rings) has a somewhat higher κ. There are two features needing discussion: (a) how to extract the $\omega=0$ limit, smoothing out the dip at low ω, and (b) whether the 1000-atom model has a larger $\omega=0$ value of κ.

All $\kappa(\omega)$ curves have a dip at the lowest energies, for reasons that were discussed in AF. The origin of this dip is shown numerically in Fig. 6, which plots the level-spacing distribution $q(\omega)$ defined as

$$q(\omega)=\frac{1}{\pi N(N-1)}\sum_{i\neq j}\frac{\eta}{(\omega-|\omega_i-\omega_j|)^2+\eta^2}\ . \tag{10}$$

This distribution has a dip near $\omega=0$ reminiscent of the dip in the $\kappa(\omega)$ curves. As argued in AF, this dip goes away as the system gets large. This can be seen from the rigorous identity

$$q(\omega)=\frac{N}{N-1}\int_0^\infty d\omega' p(\omega')p(\omega'+\omega) - \frac{1}{\pi(N-1)}\frac{\eta}{\omega^2+\eta^2}\ , \tag{11}$$

where $p(\omega)$ is the density of states, defined as

$$p(\omega)=\frac{1}{\pi N}\sum_i\frac{\eta}{(\omega-\omega_i)^2+\eta^2}\ . \tag{12}$$

From Eq. (11) we see that $q(\omega)$ differs from a smooth convolution of two smooth densities of states only by a subtracted Lorentzian at the origin of width η and weight $1/(N-1)$. The solid curves in Fig. 6 show the results of adding the missing Lorentzians back in.

Since the argument of AF and the results of Fig. 6 both show that the dip disappears as $N\to\infty$, therefore it is appropriate to develop a method to eliminate the dip in a physically correct or at least sensible manner. As a hypothesis, let us assume that $\kappa(\omega)$ has the form of a Drude conductivity minus a Lorentzian of width η:

$$\kappa(\omega)=\frac{\kappa_0}{1+\omega^2\tau^2}-\frac{\Delta}{1+\omega^2/\eta^2}\ . \tag{13}$$

The idea is that the first, or Drude term, represents the true ($N\to\infty$) thermal conduction. There are three unknown parameters, κ_0, Δ, and τ, which can be uniquely fitted to the three parameters of the calculated $\kappa(\omega)$, $\kappa(0)$, κ_M, and ω_M, where the last two are the maximum value of $\kappa(\omega)$ and the frequency where this maximum occurs. Closed form solutions can be found for the three parameters of Eq. (5) in terms of the three data points, which gives an automatic procedure for finding an extrapolated dc value, namely, κ_0. The results of this procedure are shown in Fig. 7 for several choices of η. Unfortunately, an η-independent answer does not emerge.

The source of the problem is that the Drude form does not describe the calculated $\kappa(\omega)$ well. The curves of Fig. 4, in the range 1 meV $<\omega<$ 4 meV agree well with a Drude form ($\kappa_0=0.43$ W/mK, $1/\tau=2.3$ meV) plus a constant background $\kappa_{BG}=0.42$ W/mK. This form extrapolates to a zero-frequency value of $\kappa_0+\kappa_{BG}=0.84$ W/mK, considerably less than the value of 0.93 W/mK

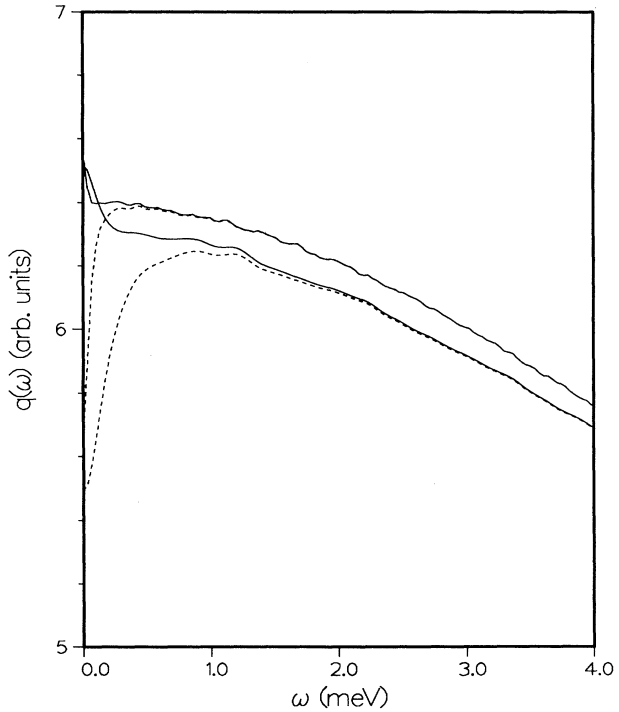

FIG. 6. Level spacing distributions. The lower curve is for model 216a with $\eta=0.172$ meV, and the upper curve for model 1000 with $\eta=0.043$ meV. Dashed curves are the correct distributions calculated from Eq. (10), and solid curves contain the missing Lorentzian part added back in.

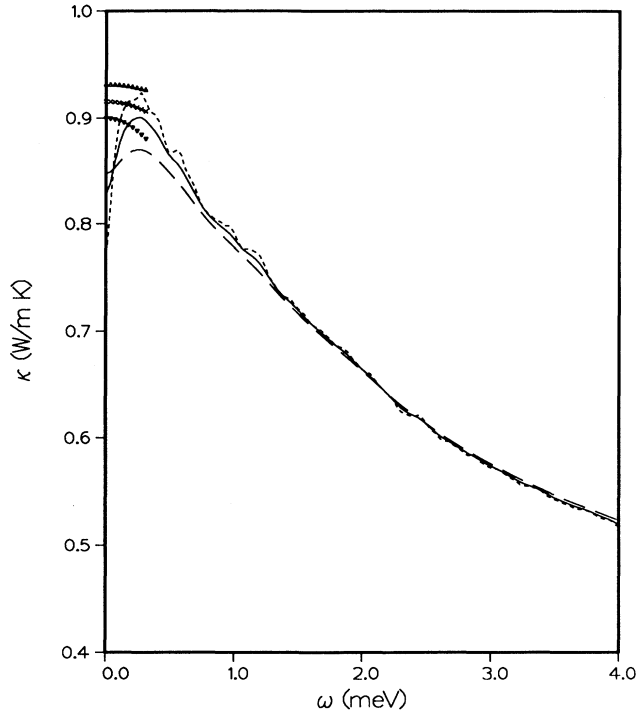

FIG. 7. Thermal conductivity vs frequency for model 1000 at $T=175$ K, calculated for three values of η, 0.043, 0.086, and 0.172 meV, and extrapolated to zero using Eq. (5).

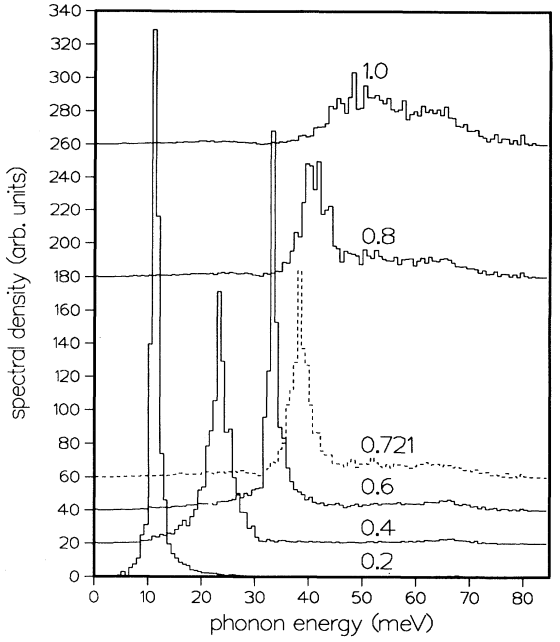

FIG. 8. Spectral density for longitudinal polarization frequency for six wave vectors. This gives the frequency spectrum needed to construct a (nonstationary) propagating state with a pure wave vector **Q** and pure longitudinal polarization [Eqs. (14) and (15)].

obtained from the automatic procedure described above and given in Fig. 7. Note that the value of 0.84 W/mK is obtained from numerical data in the range 1–4 meV independent of the choice used for η (as shown in Fig. 7) or the choice of periodic versus antiperiodic boundary conditions. This last observation tells us that the difficulty is coming from the low-ω modes, because this is the only place where boundary conditions have a significant effect. The parameters of Eq. (13) obtained by fitting to the peak of $\kappa(\omega)$ are strongly altered by the contribution of low-frequency modes, and this contribution changes with boundary condition (Fig. 4), system size (Fig. 5), and broadening parameter η (Fig. 7).

V. SPECTRAL DENSITY

Figure 8 provides further analysis of the vibrational states, and helps to illuminate the question of whether or not vibrational modes can be regarded as propagating. The spectral density for longitudinal polarization is shown versus energy for a selection of wave vectors.

$$S_L(\mathbf{Q},\omega)=\sum_i |A_i(\mathbf{Q})|^2\delta(\omega-\omega_i)\ , \tag{14}$$

$$A_i(\mathbf{Q})=\sum_l \epsilon_i(l)\cdot\hat{\mathbf{Q}}e^{i\mathbf{Q}\cdot\mathbf{R}_l}\ . \tag{15}$$

Here $A_i(\mathbf{Q})$ is the amplitude for the mode i to consist of a longitudinally polarized wave of wave vector **Q**. Figure 8 shows six wave vectors which are all reciprocal lattice vectors of the 1000-atom supercell. Five of them are of the form $(2\pi/5a)(m,0,0)$ for $m=1,2,3,4$, and 5. Since $a=5.515$ Å is almost the same as the conventional cubic cell size of crystalline diamond-structure Si (5.43 Å), these wave vectors are the counterparts to crystalline wave vectors going from near the zone center to the zone boundary in the [100] direction. The dashed curve shows a less symmetric wave vector, $(2\pi/5a)(2,3,0)$. The lowest-energy peak, at 11 meV, belongs to a wave vector $\frac{1}{5}$th of the way to the zone boundary, and would correspond to the lowest LA phonon of energy 12.5 meV that would have appeared if the atoms had been given their crystalline coordinates. If a peak in $S(\mathbf{Q},\omega)$ has a Lorentzian shape, then its full width at half maximum gives the lifetime broadening $1/\tau$. Let us define γ to be the ratio $1/\omega\tau$ where ω is the peak frequency. For the first peak in Fig. 6, $\gamma\approx 0.17$. For an acoustic mode, the ratio of mean free path to wavelength, l/λ, is $1/2\pi\gamma$, or ≈ 1 for this mode. This is consistent with the finding of Love and Anderson[9] that for a-SiO_2, states with $\omega>4$ meV have $l\approx\lambda$. The second peak in Fig. 8 has about the same value of γ, whereas the third peak has narrowed, corresponding to the diffusivity peak in Fig. 2 at 31–35 meV. This peak sits on a broader background than is found in the first two peaks, but has a very narrow Lorentzian component with a lifetime at least as long as the first peak. A group velocity can be assigned by taking a slope of a graph of peak frequency versus wave vector. This velocity ($\approx 7\times 10^5$ cm/sec) is slightly smaller than the acoustic velocity seen at smaller **Q**'s. The mean free path is about the same as for the first peak, namely, the cell size. At larger wave vectors there is a dramatic change in the spectral shape. Insofar as they can be

defined, full widths at half maximum are 30–60 % of the peak frequency, which corresponds to mean free paths (with a generous choice of acoustic velocities) a factor of 2 or more smaller than the corresponding crystalline wavelengths. Clearly the modes at the lower end of the spectrum are marginally propagating, whereas the majority of modes, which lie in the upper half of the spectrum of energies and wave vectors, are not propagating in any sense. Nevertheless, they are extended, diffusive, and contribute a significant heat current.

VI. EFFECT OF MASS DISORDER

Our results for pure a-Si provide support and interpretation for the notion of "minimum thermal conductivity." It is both disappointing and surprising that this concept should seem so robust. The disappointment is that one would like to be able to create better thermal insulators than a-Si, while still preserving the ability to carry electrical currents. This could improve the performance of thermoelectric devices. The surprise is that diffusive behavior should be found for nearly all vibrational modes even though $l \approx a$. It is important to ask how much additional disorder is needed to push states over the mobility edge into the localized regime, and also to ask whether the mode diffusivities D_i of the diffusive states are pinned near a value $D_i \approx \frac{1}{3}va$, or can this value be continuously diminished by adding further disorder.

To answer these questions it is very natural to enhance artificially the degree of disorder of a-Si by randomly changing a fraction x of the masses from the Si mass (28 amu) to the germanium mass (73 amu), leaving atomic positions and force constants unchanged. Obviously, this can be regarded as a model for the behavior of an amorphous $Si_{1-x}Ge_x$ alloy, although in actual alloys there is no guarantee that the topological disorder or the force constants remain independent of x. Crystalline $Si_{1-x}Ge_x$ alloys have been much studied, and it is clear that simple models like rigid band or virtual crystal are not adequate for understanding electron behavior.[32] Since electron

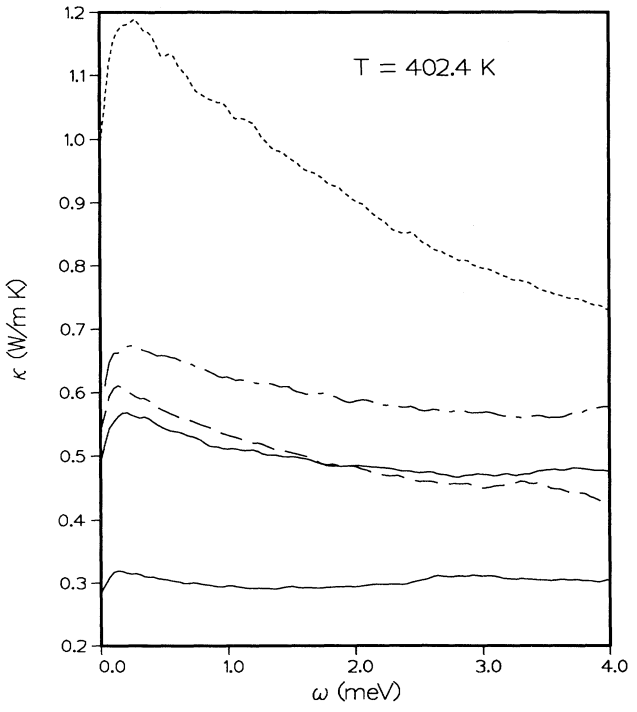

FIG. 9. Frequency-dependent thermal conductivity of various alloys $Si_{1-x}Ge_x$ at 400 K. Small dashed line: $x=0$; broken line: $x=0.25$; upper solid line: $x=0.50$; long dashed line: $x=0.75$; lower solid line: $Si_{0.5}Ge^*_{0.5}$. Lorentzian broadening $\eta=0.043$ meV.

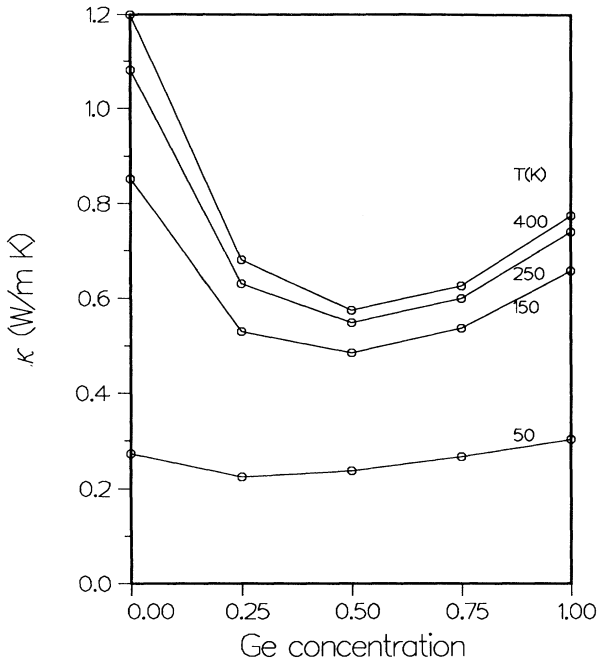

FIG. 10. Ge concentration dependence of the thermal conductivity of Si-Ge alloys at selected temperatures.

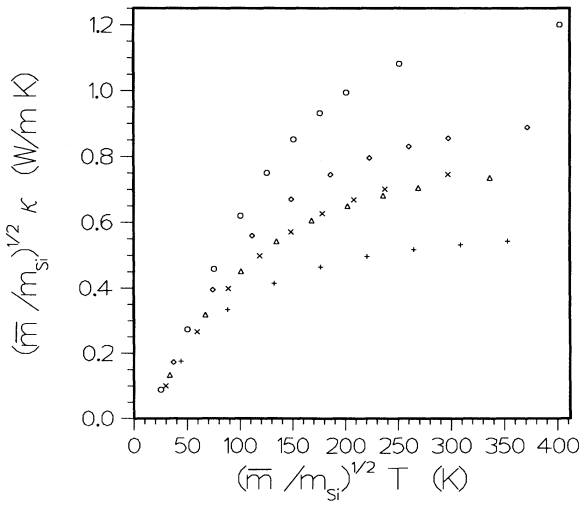

FIG. 11. Scaled thermal conductivity vs scaled temperature for various alloys $Si_{1-x}Ge_x$. Circles: $x=0$ and $x=1$; crosses: $x=0.25$; triangles: $x=0.50$; diamonds: $x=0.75$; +'s: $Si_{0.5}Ge^*_{0.5}$.

response determines force constants, this suggests that force constants in the amorphous alloys will change in complicated ways. Nevertheless, it is reasonable to believe that mass disorder is the dominant new effect, as has been argued in the context of thermal conductivity studies of crystalline $Si_{1-x}Ge_x$ alloys.[33] This is supported by the fact that radial distribution functions of amorphous germanium and silicon are very similar.[34] We have studied the three cases $x=(0.25,0.50,0.75)$ and also a case where $x=0.50$ and the impurity mass is 145 amu, twice the germanium mass. This hypothetical heavy germanium atom will be denoted by Ge*. Our results for $N(\omega)$ and $1/p$ are very similar to those of Bouchard *et al.*[35] These in turn compare quite well with Raman data,[36] providing further evidence for the realism of this model.

Figure 9 shows the frequency dependence of the thermal conductivity for several Ge concentrations, as well as 50% Ge*, but at a single temperature (400 K). As before, all results are averaged over boundary conditions and Cartesian components. Figure 10 compiles the extrapolated zero-frequency results as a function of Ge composition. Unlike the case of Fig. 1 for pure *a*-Si, no effort

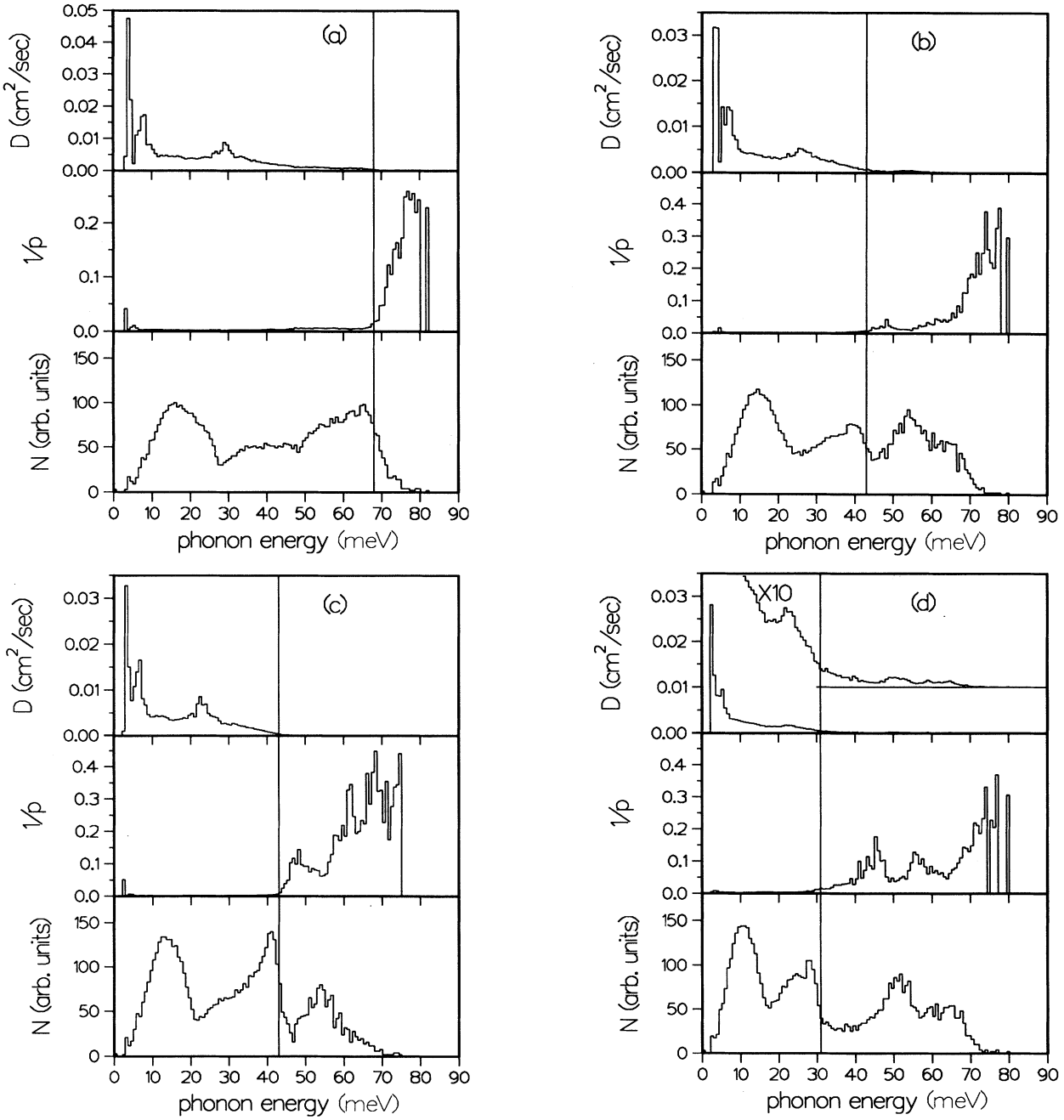

FIG. 12. Vibrational densities of states, diffusivities, and inverse participation ratios for $Si_{1-x}Ge_x$ alloys. (a) $x=0.25$; (b) $x=0.50$; (c) $x=0.75$; (d) $Si_{0.5}Ge^*_{0.5}$.

has been made to estimate the additional heat current coming from the long wavelength modes omitted in our finite-size calculations. These are our "raw data," a lower bound on the total. Note that if the "minimum conductivity" idea were robust, i.e., if structural disorder were large enough that additional disorder could not cause additional decrease of conductivity, then contrary to Fig. 10, monotonic behavior would have occurred. This is amplified below.

A virtual crystal model was developed by Abeles[37] for the thermal conductivity of crystalline Si-Ge alloys. Individual atomic masses are replaced by an average mass, $\overline{m}=(1-x)m_{\mathrm{Si}}+xm_{\mathrm{Ge}}$. If the "minimum conductivity" model and the virtual crystal model were both correct, thermal conductivity would scale in a very simple way with the scaling parameter

$$s=\sqrt{\overline{m}/m_{\mathrm{Si}}}\ . \tag{16}$$

Since each mode would have its frequency ω_i scaled to ω_i/s, the molar specific heat would be just the value for the pure ($x=0$) material, C_0 at a scaled temperature $C(T)=C_0(sT)$. The only T dependence of $\kappa=\frac{1}{3}Cva$ is the T dependence of C, and the only other mass dependence is in the velocity which becomes v/s. Thus we would get $s\kappa(sT)=\kappa_0(T)$, where κ_0 is the $x=0$ result for pure a-Si. This scaling is rigorously obeyed at the pure Ge endpoint $x=1$, and is tested for the various alloys in Fig. 11. At low temperatures all the scaled results lie on the same curve, but for scaled temperature $sT\geq 80$ K there is a significant effect of mass disorder. Contrary to the notion of "minimum conductivity," these results demonstrate a systematic increase of the scaled thermal resistivity with increasing mass disorder. In crystalline Ge, Geballe and Hull[38] measured the shift of $\kappa(T)$ caused by isotope mass disorder. In Boltzmann theory one finds that the thermal resistivity should have an additive term proportional to $\langle(1/m-\langle 1/m\rangle)^2\rangle$. Our $T=402$ K results, for example, can be shown to be crudely consistent with this effect except smaller by an order of magnitude than what would have followed by scaling the crystalline Ge results.

These results can be understood in more detail by examining the properties of the vibrational eigenstates as shown in Fig. 12. Not surprisingly, mass disorder enlarges the region of localized modes at the upper end of the spectrum, and diminishes the diffusivity of the delocalized modes in the middle of the spectrum. These calculations permit quite a reliable determination of the mobility edge ω_c. In pure a-Si (Fig. 1), $\omega_c\approx 71$ meV; in the alloy $Si_{0.75}Ge_{0.25}$, $\omega_c\approx 68$ meV, while for both $Si_{0.5}Ge_{0.5}$ and $Si_{0.25}Ge_{0.75}$, $\omega_c\approx 43$ meV; and in $Si_{0.5}Ge^{*}_{0.5}$, $\omega_c\approx 31$ meV. Figures 1 and 12 show a small number of low-energy states with enhanced values of $1/p$. However, these are not true localized states, for when we change boundary conditions from periodic to antiperiodic, the values of $1/p$ for the high-energy localized states are almost unchanged, but values of $1/p$ for low-ω states are affected. We agree with Bouchard *et al.*[35] that the presence of threefold coordinated atoms enhances the value of $1/p$ at low ω.

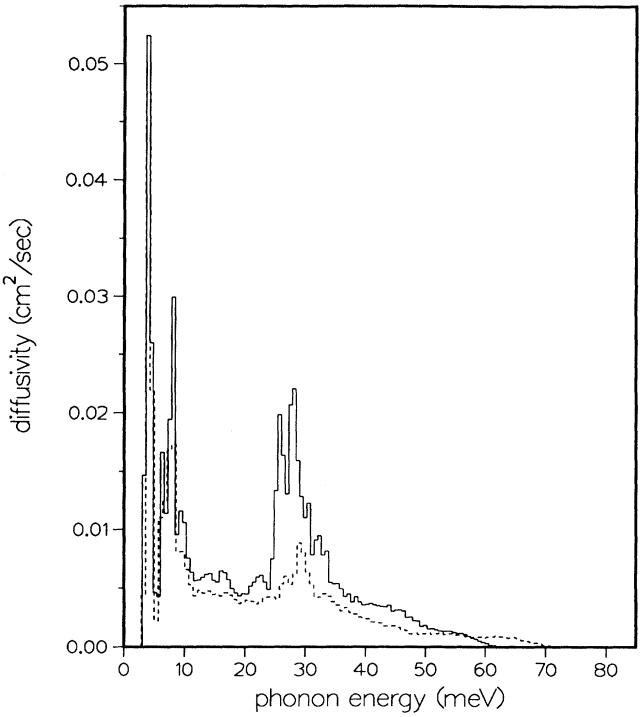

FIG. 13. Diffusivity for amorphous $Si_{0.75}Ge_{0.25}$ (dashed) compared with the scaled ("virtual crystal") result (solid) based on a-Si.

The trends in the value of ω_c can be understood in a simple way. Light mass defects, as occur in $Si_{0.25}Ge_{0.75}$, lead to localized modes, and heavy mass defects, as occur in $Si_{0.75}Ge_{0.25}$, lead to resonant modes which are not localized. Thus adding small amounts of Ge to pure amorphous Si does not perturb ω_c far from the pure Si mobili-

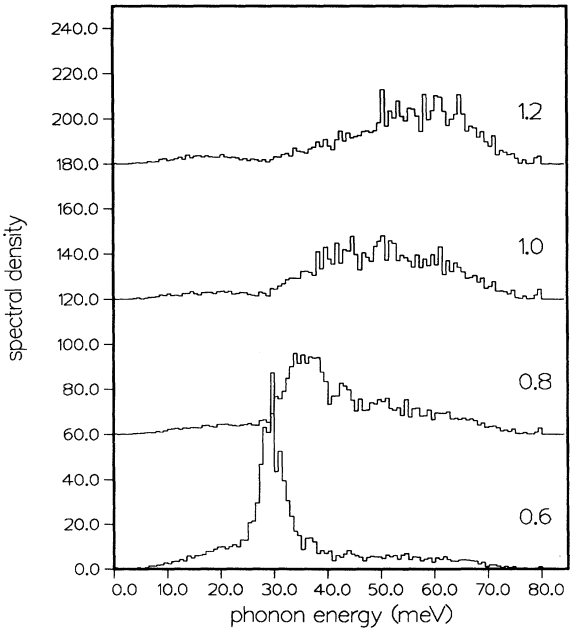

FIG. 14. Spectral functions for amorphous $Si_{0.75}Ge_{0.25}$ for comparison with Fig. 8 for pure a-Si.

ty edge, as seen in $Si_{0.75}Ge_{0.25}$. Our model for pure a-Ge is identical to pure a-Si except all frequencies are scaled down by the square root of the mass ratio, i.e., $\omega_c \approx 44$ meV. Adding Si to pure amorphous Ge introduces new localized states above the mobility edge of pure amorphous Ge, but as seen in $Si_{0.25}Ge_{0.75}$ and $Si_{0.5}Ge_{0.5}$, this does not shift the position of the mobility edge. Apparently the location of ω_c moves abruptly from the pure Si value of 71 meV to the pure Ge value of 44 meV somewhere between $Si_{0.75}Ge_{0.25}$ and $Si_{0.5}Ge_{0.5}$.

Besides the effect of localized states at high energies, the additional disorder caused by mass substitutions cause a decrease in diffusivity of the delocalized states which is greater than would be predicted by the formula $D \approx \frac{1}{3}va$ and simple mass scaling. This is shown in Fig. 13. Figure 14 shows some spectral functions, for $Si_{0.75}Ge_{0.25}$, which are significantly broader than the ones shown for pure a-Si in Fig. 8. This agrees with modern ideas about the Anderson transition being continuous, but is in apparent conflict with the empirical idea of a minimum conductivity. It seems to us that the resolution of this conflict is the human tendency to perceive "universal" aspects even of accidental events. Apparently, naturally disordered systems like glasses tend to occur with $D \approx \frac{1}{3}va$. We see no reason why this should occur, except for observing that the crossover between propagating and localized states tends to be broad and gradual. Seeing no dramatic deviations from this rule, normal custom leads to the loose label "universal."

ACKNOWLEDGMENTS

We thank X. P. Li for the harmonic phonon programs used in this work. We thank J. Sethna and H. Smith for a very helpful correspondence drawing our attention to the divergence of κ in harmonic approximation. M.D.K. thanks the National Research Council for support. Calculations were performed on the IBM 3090 machine at the Cornell Supercomputer Center. F.W. thanks Lawrence Livermore Laboratories for partial support. Work at Stony Brook was supported in part by NSF Grant No. DMR-9118414.

[1]G. Pompe and E. Hegenbarth, Phys. Status Solidi B **147**, 103 (1988).

[2]D. G. Cahill, H. E. Fischer, T. Klitsner, E. T. Swartz, and R. O. Pohl, J. Vac. Sci. Technol. A **7**, 1259 (1989).

[3]R. C. Zeller and R. O. Pohl, Phys. Rev. B **4**, 2029 (1971).

[4]P. W. Anderson, B. I. Halperin, and C. M. Varma, Philos. Mag. **25**, 1 (1972); W. A. Phillips, J. Low Temp. Phys. **7**, 351 (1972).

[5]P. B. Allen and J. L. Feldman, preceding paper (denoted AF), Phys. Rev. B **48**, 12 581 (1993).

[6]C. Kittel, Phys. Rev. **75**, 972 (1948); F. Birch and H. Clark, Am. J. Sci. **238**, 613 (1940); P. W. Bridgman, Proc. Am. Acad. **59**, 141 (1923).

[7]G. A. Slack, in *Solid State Physics,* edited by H. Ehrenreich, F. Seitz, and D Turnbull (Academic, New York, 1979), Vol. 34, p. 1.

[8]P. Sheng and M. Zhou, Science **253**, 539 (1991).

[9]M. S. Love and A. C. Anderson, Phys. Rev. B **42**, 1845 (1990).

[10]A. Jagannathan, R. Orbach, and O. Entin-Wohlman, Phys. Rev. B **39**, 13 465 (1989).

[11]J. Michalski, Phys. Rev. B **45**, 7054 (1992).

[12]D. N. Payton, M. Rich, and W. M. Visscher, Phys. Rev. **160**, 706 (1967).

[13]F. H. Stillinger and T. A. Weber, Phys. Rev. B **31**, 5262 (1985).

[14]R. van den Berg and H. v. Löhneysen, Phys. Rev. Lett. **55**, 2463 (1985).

[15]F. Wooten, K. Winer, and D. Weaire, Phys. Rev. Lett. **54**, 1392 (1985).

[16]P. N. Keating, Phys. Rev. **145**, 637 (1966).

[17]R. E. Cowley, Phys. Rev. Lett. **60**, 2379 (1988).

[18]X.-P. Li, G. Chen, P. B. Allen, and J. Q. Broughton, Phys. Rev. B **38**, 3331 (1988).

[19]P. B. Allen and J. L. Feldman, Phys. Rev. Lett. **62**, 645 (1989); **64**, 2466(E) (1990); J. L. Feldman and P. B. Allen, Mat. Res. Soc. Symp. Proc. **141**, 219 (1989).

[20]J. L. Feldman, J. Q. Broughton, P. B. Allen, and F. Wooten, in *Proceedings of the 20th International Conference on the Physics of Semiconductors,* edited by E. M. Anastassakis and J. D. Joannopoulos (World Scientific, Singapore, 1990), p. 2075.

[21]G. N. van der Hoven, Z. N. Liang, L. Niesen, and J. S. Custer, Phys. Rev. Lett. **68**, 3714 (1992).

[22]W. A. Kamitakahara, C. M. Soukoulis, H. R. Shanks, U. Buchenau, and G. S. Grest, Phys. Rev. B **36**, 6539 (1987).

[23]J. L. Feldman, J. Q. Broughton, and F. Wooten, Phys. Rev. B **43**, 2152 (1991).

[24]P. A. Lee and T. V. Ramakrishnan, Rev. Mod. Phys. **57**, 287 (1985).

[25]R. Biswas, A. M. Bouchard, W. A. Kamitakahara, G. S. Grest, and C. M. Soukoulis, Phys. Rev. Lett. **60**, 2280 (1988); Y. H. Lee, R. Biswas, C. M. Soukoulis, C. Z. Wang, C. T. Chan, and K. M. Ho, Phys. Rev. B **43**, 6573 (1991).

[26]U. Buchenau, Yu. M. Galperin, V. L. Gurevich, D. A. Parshin, M. A. Ramos, and H. R. Schober, Phys. Rev. B **46**, 2798 (1992); M. García-Hernández, R. Burriel, F. J. Mermejo, C. Piqué, and J. L. Martínez, J. Phys. Condens. Matter **4**, 9581 (1992).

[27]J. K. Flicker and P. L. Leath, Phys. Rev. B **7**, 2296 (1973).

[28]S. Hunklinger and W. Arnold, in *Physical Acoustics,* edited by W. P. Mason and R. N. Thurston (Academic, New York, 1976), Vol. 12, p. 155.

[29]M. Mertig, G. Pompe, and E. Hegenbarth, Solid State Commun. **49**, 369 (1984).

[30]Reviews are given by P. B. Allen, in *Superconductivity in d- and f-Band Metals,* edited by H. Suhl and M. B. Maple (Academic, New York, 1980), p. 291; in *Physics of Transition Metals, 1980,* edited by P. Rhodes (IOP, London, 1981), p. 425.

[31]D. G. Cahill, S. K. Watson, and R. O. Pohl, Phys. Rev. B **46**, 6131 (1992).

[32]S. de Gironcoli, Phys. Rev. B **46**, 2412 (1992); S. de Gironcoli, P. Pavone, and S. Barone, Phys. Rev. B **43**, 7231 (1991).

[33]B. Abeles, D. S. Beers, G. D. Cody, and J. P. Dismukes, Phys. Rev. **125**, 44 (1962).

[34]J. M. Holender and G. J. Morgan, J. Phys. Condens. Mater. **3**,

7241 (1991); J. Fortner and J. S. Lannin, Phys. Rev. B **39**, 5527 (1989); G. Etherington, A. C. Wright, J. T. Wenzel, J. C. Dore, J. H. Clarke, and R. N. Sinclair, J. Non-Cryst. Sol. **48**, 265 (1982).

[35]A. M. Bouchard, R. Biswas, W. A. Kamitakahara, G. S. Grest, and C. M. Soukoulis, Phys. Rev. B **38**, 10499 (1988).

[36]J. S. Lannin, in *Amorphous and Liquid Semiconductors* (Taylor and Francis, London, 1974), p. 1245.

[37]B. Abeles, Phys. Rev. **131**, 1906 (1963).

[38]T. H. Geballe and G. W. Hull, Phys. Rev. **110**, 773 (1958).